NAVAL AIR WARFARE CENTER AIRCRAFT DIVISION
PATUXENT RIVER, MARYLAND

TECHNICAL INFORMATION MEMORANDUM

REPORT NO: NAWCADPAX/TIM-2017/2

NICKEL INTERLAYER COATING AND HYDROGEN EMBRITTLEMENT

by

E.U. Lee
M. Stanley
B. Pregger

23 February 2021

DISTRIBUTION STATEMENT A. Distribution authorized for public release.

DEPARTMENT OF THE NAVY
NAVAL AIR WARFARE CENTER AIRCRAFT DIVISION
PATUXENT RIVER, MARYLAND

NAWCADPAX/TIM-2017/2

NICKEL INTERLAYER COATING AND HYDROGEN EMBRITTLEMENT

by

E.U. Lee
M. Stanley
B. Pregger

RELEASED BY:

BRENNAN.JOHN.E.1292869335 Digitally signed by BRENNAN.JOHN.E.1292869335 Date: 2021.03.03 08:56:48 -05'00'

JOHN BRENNAN 23 FEBRUARY 2021
Head, Materials Engineering Division
Naval Air Warfare Center Aircraft Division

CONTROLLED UNCLASSIFIED INFORMATION

REPORT DOCUMENTATION PAGE

Form Approved
OMB No. 0704-0188

Public reporting burden for this collection of information is estimated to average 1 hour per response, including the time for reviewing instructions, searching existing data sources, gathering and maintaining the data needed, and completing and reviewing this collection of information. Send comments regarding this burden estimate or any other aspect of this collection of information, including suggestions for reducing this burden, to Department of Defense, Washington Headquarters Services, Directorate for Information Operations and Reports (0704-0188), 1215 Jefferson Davis Highway, Suite 1204, Arlington, VA 22202-4302. Respondents should be aware that notwithstanding any other provision of law, no person shall be subject to any penalty for failing to comply with a collection of information if it does not display a currently valid OMB control number. **PLEASE DO NOT RETURN YOUR FORM TO THE ABOVE ADDRESS.**

1. REPORT DATE	2. REPORT TYPE	3. DATES COVERED
2017	Technical Information Memorandum	Jan 2016 to Jan 2017

4. TITLE AND SUBTITLE

NICKEL INTERLAYER COATING AND HYDROGEN EMBRITTLEMENT

5a. CONTRACT NUMBER

5b. GRANT NUMBER

5c. PROGRAM ELEMENT NUMBER

6. AUTHOR(S)

E.U. Lee
M. Stanley
B. Pregger

5d. PROJECT NUMBER

5e. TASK NUMBER

5f. WORK UNIT NUMBER

7. PERFORMING ORGANIZATION NAME(S) AND ADDRESS(ES)
Naval Air Warfare Center Aircraft Division
Bldg. 2188 12345 48066 Shaw Road

8. PERFORMING ORGANIZATION REPORT NUMBER

NAWCADPAX/TIM-2017/2

9. SPONSORING/MONITORING AGENCY NAME(S) AND ADDRESS(ES)
OSD Demonstration Projects
US NAVY Lemieux, Edward J
NRL Washington D.C. 20670-1547

10. SPONSOR/MONITOR'S ACRONYM(S)

11. SPONSOR/MONITOR'S REPORT NUMBER(S)

12. DISTRIBUTION/AVAILABILITY STATEMENT

DISTRIBUTION STATEMENT A. Distribution authorized for public release.

13. SUPPLEMENTARY NOTES

14. ABSTRACT

A study was conducted to clarify the effect of Ni interlayer on the hydrogen embrittlement of M54 steel, coated with Cd or (Zn-14%Ni). Ni interlayer induced a loss of threshold stress intensity for environmental hydrogen embrittlement $K_{th\text{-}EHE}$ or a loss of resistance to hydrogen embrittlement. This is attributed to the blockage of egress and entrapment of hydrogen, absorbed during coating process. The post-coating baking in air was able to prevent the hydrogen embrittlement partially, but not completely. On the other hand, the coating Cd or (Zn-14%Ni) with or without Ni interlayer protected the substrate M54 steel from corrosion fatigue in a 3.5% NaCl solution.

15. SUBJECT TERMS

16. SECURITY CLASSIFICATION OF:			17. LIMITATION OF ABSTRACT	18. NUMBER OF PAGES	19a. NAME OF RESPONSIBLE PERSON
a. REPORT	b. ABSTRACT	c. THIS PAGE			19b. TELEPHONE NUMBER (include area code)
Unclassified	Unclassified	Unclassified	SAR		

Standard Form 298 (Rev. 8-98)
Prescribed by ANSI Std. Z39-18

SUMMARY

Ferrium M54 steel specimens were coated with either Cadmium (Cd) or Zinc (Zn)-14% Nickel (Ni) The influence of a Ni interlayer beneath these coatings was investigated by preparing specimens with and without the Ni interlayer coating. The specimens were subjected to examinations of microstructure and fractograph, measurement of electrochemical polarization, and tests of tension, fatigue, and hydrogen embrittlement. The microstructure of the substrate M54 steel was tempered martensite plates with carbide particles on the plate boundaries. The corrosion potentials or open circuit potentials were measured to be -0.53v and -0.78v for the bare and Cd plus Ni interlayer coated, respectively. This indicates that the coating became more active and sacrificial. The tensile strengths of the bare and coated specimens were similar, indicating that the there is little or no coating effect on the tensile strength. In air, the fatigue strength was reduced by coating with or without Ni interlayer. On the other hand, in 3.5% NaCl solution, the reverse was true, indicating the protective action of the coating against corrosion fatigue. The threshold stress intensity for environmental hydrogen embrittlement $K_{th\text{-}EHE}$ was greatest for the bare specimen and it was lost by coating. The loss was greatest for the Cd plus Ni interlayer coating. The lost $K_{th\text{-}EHE}$ of the coated specimen was restored to a certain limit by baking. Under slow strain rate testing, the fracture strength in 3.5% NaCl solution was lower for the specimen coated with Ni interlayer than for its absence. This suggests that the Ni interlayer reduced the hydrogen embrittlement resistance more in 3.5% NaCl solution.

CONTROLLED UNCLASSIFIED INFORMATION

Contents

CONTROLLED UNCLASSIFIED INFORMATION

ACKNOWLEDGEMENTS

The authors gratefully acknowledge the support of this study, Index W15NA05, by the Office of Secretary of Defense. Special thanks are due to Mr. Stephen J. Spadafora of lEIDOS and Mr. Dane C. Hanson of NAWCADPAX for providing technical guidance and monitoring.

INTRODUCTION

BACKGROUND

It is known that electroplating causes atomic hydrogen to be absorbed by the steel substrate, producing delayed failure by direct-embrittlement by hydrogen. Hydrogen is also absorbed when a sacrificial coating undergoes corrosion in service, and this process is known as re-embrittlement. The level of re-embrittlement susceptibility is associated with the electro-negativity and the barrier properties of the plating.

The hydrogen embrittlement of a 4340 steel, induced by Zn-Co electroplating, was studied by Hillier in 2001 (reference 1). The embrittlement was found to be less severe than that caused by Cd or Zn electroplating. The mechanical properties of Zn-Co electroplated specimens were not fully regained by standard baking treatments. Increasing the baking period to 48 hours from 24 hours only increased the recovery from 89 to 91%. On the other hand, the Zn-Ni electroplating induced the least embrittlement of the single layer plating. This finding was attributed to the formation of an enriched Ni layer at the plating/substrate interface that had a low hydrogen diffusivity.

The susceptibility of high strength steels to direct-embrittlement and re-embrittlement was studied by Figueroa Gordon in 2005 (reference 2). In this study, the effects of Cd, Zn-14% Ni and Al based SermeTel 1140/962 electroplatings on those embrittlements of 300M, AerMet 100, GifloM2000 and CSS-42L steels were investigated and compared. AerMet 100 steel showed less susceptibility to those embrittlements among the steels tested.

Lee and his co-workers of NAWCADPAX studied the effects of three coating systems on the mechanical property, fatigue, and stress corrosion cracking (SCC) of 4340 steel in 2013 (reference 3). The three coating systems were electroplated Cd and chromate passivation, Cd with chromate primer, and Cd, chromate primer and polyurethane topcoat. The three coating systems reduced the bending strength and hardness of the base metal 4340 steel in air. The respective effects on the fatigue resistance of bare 4340 steel were similar in air and 3.5% NaCl solution. In addition, they were found to reduce the fatigue resistance of 4340 steel in air, but protect the substrate partly from aggressive environmental attack in 3.5% NaCl solution. The reduction of bending strength, hardness and fatigue resistance in air is attributed to hydrogen embrittlement, induced by Cd-electroplating. The SCC resistance was found to be enhanced more by each additional coating on the initial electroplated Cd.

Lee and his coworkers also studied bare and Zn-14% Ni electroplated M54 steels to clarify their mechanical, fatigue and SCC properties in 2015 (reference 4). Compared to AerMet 100 steel, M54 steel has much greater SCC/hydrogen embrittlement resistance in 3.5% NaCl solution, but similar mechanical properties and susceptibility to corrosion fatigue in 3.5% NaCl solution. The Zn-14% Ni plating appears to provide the steel some protection against corrosion fatigue in 3.5% NaCl solution. The fatigue crack growth mechanisms of the bare and coated steels are striation formation in air, and a combination of striation formation and intergranular SCC in 3.5% NaCl solution.

CONTROLLED UNCLASSIFIED INFORMATION

During the aforementioned study on hydrogen re-embrittlement susceptibility of high strength steels at Cranfield University, U. K. (reference 2), GifloM2000 steel specimens were inadvertently coated thinly with Ni beneath the main Cd electroplating. Subsequently, the specimens were found to be not susceptible to hydrogen re-embrittlement. The analysis at the steel-Cd interface showed Ni content up to 7.5% compared to 1.5% in the substrate steel. The lack of hydrogen re-embrittlement in 3.5% NaCl solution is attributable to the accidently applied thin Ni layer acting as an effective barrier to hydrogen generated by the corrosion of the Cd. Ni has a very low hydrogen diffusivity $8x10^{-10}$ cm^2/s compared to $4x10^{-8}$ cm^2/s for GifloM2000 steel. In addition, it was hypothesized that a thinner Ni layer could be more effective than a thicker one in preventing hydrogen absorption, since the hydrogen diffusivity decreases with decreasing plating thickness. This could have important implications. A thin Ni layer beneath the sacrificial coating seems to be the answer to both direct-embrittlement and re-embrittlement problems. To validate and demonstrate this hypothesis, this study is proposed.

PURPOSE

The purpose of this project is to clarify the necessity of interlayer coating for possible prevention/mitigation of hydrogen embrittlement, identify the effectiveness of post-coating baking for the prevention/mitigation of hydrogen embrittlement, and establish the mechanism of prevention/mitigation of hydrogen embrittlement by interlayer coating and post-coating baking.

METHODS

HYPOTHESES

- An interlayer of low hydrogen diffusivity beneath a sacrificial coating can block hydrogen diffusion into the substrate and prevent/mitigate hydrogen embrittlement, induced by electroplating.
- Effective removal of hydrogen in coating & substrate can prevent/mitigate the hydrogen embrittlement.

EXPERIMENTAL APPROACH

MATERIALS

A forged square bar of M54 steel, 4 x 4 x 24 in., was supplied by Latrobe Specialty Metals Co., Latrobe, PA. The typical chemical composition of the steel is shown in Table B-1, and the microstructure in Figure A-1. The steel was heat-treated by Hercules Heat Treating Corp., Brooklyn, NY as follows: solution-treating at 1940oF (1060oC) for 60-90 min, oil quenching, freezing at -100oF (-73oC) for 1-3 hour, air warming, tempering at 960oF (516oC) for 10 hours, and air cooling.

Electrodeposits of Cd are used to protect steel and cast iron against corrosion. Because Cd is anodic to iron, the underlying ferrous metal is protected at the expense of the Cd plate even if the Cd becomes scratched or nicked, exposing the substrate. Cd is usually applied as a thin coating

(less than 25 μm thick) intended to withstand atmospheric corrosion. It is seldom used as an undercoating for other metals, and its resistance to corrosion by most chemicals is low. Besides having excellent corrosion protective properties, Cd has many useful engineering properties, including natural lubricity. When corrosion products are formed on Cd-electroplated parts, they are not voluminous, and there is minimal change in dimension. These two properties are responsible for the wide use of Cd on moving parts or threaded assembles. Cd has excellent electrical conductivity and low contact resistance. However, Cd is highly toxic, and health, safety, and environmental concerns are driving the reduction or elimination of its use for many applications. Cd is used as one of the coating materials in this study.

Zn-Ni alloys are reported to produce the highest corrosion resistance of the electroplated Zn alloys, and the corrosion resistance on steel increasing with Ni content up to 15 to 18% (reference 1). Beyond this range the alloy becomes more noble than steel and loses its sacrificial protection property. Therefore, Zn-14% Ni alloy was selected as one of the coating materials in this study.

SPECIMENS

The square bar M54 steel was machined to the following specimens:

- round tension test specimen of gage length 1 in. and diameter 0.25 in. in S-orientation for tension test (ASTM E8) and slow strain rate test (ASTM G129)
- hourglass specimen of minimum diameter 0.25 in. in S-orientation for stress-life fatigue test (ASTM E466)
- square bar specimen of 0.4 x 0.4 x 2.8 in. in S-L orientation with a Charpy notch at the mid-length for SCC test under four-point bending (ASTM F 1624)
- flat plate specimen of 4x4x1/8 in. for electrochemical polarization experiment

COATING

The Cd with Ni interlayer coating and the subsequent baking at 375^{o}F were done by Gramatic Platers, Inc., Tenafly, N. J.

The Zn-14% Ni alloy with Ni interlayer coating was carried out, following the alkaline LHE (low hydrogen embrittlement) Zn-Ni alloy plating process, DIPSOL IZ-C17+ (reference 5). This process was approved for the U. S. Air Force Drawing 201027456 high strength steel applications, and meets Boeing BAC5637 and AMS 2417 specifications for low strength steel and other substrates. It also meets the requirements for a non-embrittling process per ASTM F519. The post-coating baking was done at 375^{o}F in air.

CONTROLLED UNCLASSIFIED INFORMATION

ELECTROCHEMICAL POLARIZATION MEASUREMENT

The electrochemical behavior of the coated M54 steel was characterized by conducting polarization experiment in aqueous 3.5% NaCl solution of pH 7.3. For this experiment, a specimen was mounted in a flat cell that would expose a circular 0.2 in^2 area to the solution. Before the start of the polarization experiment, the specimen was allowed to freely corrode in the NaCl solution under open-circuit condition until a steady-state potential was reached. For the polarization experiment, the potential of the specimen with respect to the SCE was controlled with a SI 1287 Potentiostat/Galvanostat from 100 mV below the free corrosion potential, while the current required to maintain the potential of the specimen was recorded. The corrosion current was estimated through linear polarization resistance measurements using scans from 100 mV below to 100mV above at a scan rate of 0.167 mV/s.

TESTS

Tension Test
A closed-loop servo-hydraulic mechanical test machine, Interlaken, of 20 kip (90 KN) capacity was utilized for the tension test. The test was conducted with the tension test specimen in air, following the ASTM E 8 – 01, Standard Test Methods for Tension Testing of Metallic Materials. The tensile loading rate was 0.003 in/min (0.076 mm/min).

Stress-Life Fatigue Test
This test was also carried out in the Interlaken of 20 kip (90 KN) capacity, employing the hourglass specimen, under stress control in tension-tension cycling at stress ratio 0.1 and frequency 10 Hz in air and aqueous 3.5% NaCl solution of pH 7.3. This test followed the ASTM E 466 – 96, Standard Practice for Conducting Force Controlled Constant Amplitude Axial Fatigue Tests of Metallic Materials.

Hydrogen Embrittlement Tests
Two test methods, rising step load (RSL) and slow strain rate (SSR), were used to quantify the degree of hydrogen embrittlement produced in bare and coated M54 steel specimens during exposure to aqueous 3.5% NaCl solution of pH 7.3.

Rising Step Load (RSL) Test
Since the cantilever bend or double cantilever beam test takes a long time, an accelerated hydrogen embrittlement test was conducted in a RSL 1000 SI-Multi-Mode Test System (reference 6). This System included a bending frame, a tensile loading frame, an electrolyte reservoir, a pump for electrolyte circulation, a SCE, a platinum counter-electrode, a PC and a printer. The specimen, not pre-cracked, was step-loaded until the load dropped in four-point bending under constant displacement control, while held at a given potential in aqueous 3.5% NaCl solution of pH 7.3. The load drop corresponds to the threshold stress intensity for environmental hydrogen embrittlement, $K_{th\text{-}EHE}$, at a given cathodic potential.

CONTROLLED UNCLASSIFIED INFORMATION

Slow Strain Rate (SSR) Test
The test was performed in a tensile loading frame at a strain rate, varying from 10^{-8} to 10^{-4} s^{-1}, in two environments, air and 3.5% NaCl solution, respectively. The specimen for the test in NaCl solution was placed in an environmental chamber, which contained aqueous 3.5% NaCl solution of pH 7.3 enough to completely immerse the gage section of the specimen. During the test, the NaCl solution was continuously circulated between the environmental chamber and the reservoir by a pump. The specimen was pulled in tension to fracture, and the fracture strength was recorded. The difference between the values of fracture strength, acquired in air and NaCl solution, was taken as a measure of the environmental hydrogen embrittlement.

FRACTOGRAPHY

After the tension, bending, and corrosion resistance tests, the representative fracture surfaces of the specimens were examined with a JEOL JSM-6460LV scanning electron microscope, operated at an accelerating voltage of 20 kV.

EXPERIMENTAL RESULTS

MICROSTRUCTURE
The optical micrograph of the M54 steel, Figure A-1, shows tempered martensite plates with carbide particles precipitated on their boundaries.

ELECTROCHEMICAL CHARACTERISTICS
The polarization plots for the bare and coated M54 steel specimens are shown in Figure A- 2. The corrosion potential E or open circuit potential (OCP) was found to be -0.53v and

-0.78v for the bare and Cd with Ni interlayer coated specimens, respectively.

SEM FRACTOGRAPHS OF BARE AND COATED SPECIMENS
Figure A-3 shows the SEM fractographs of the single-edge-notched bare, Cd-coated, and Cd with Ni interlayer coated square bar specimens, which were fractured under four-point bending in air. The coated specimens were subjected to post-coating baking at 375ºF for 4 hours in air. Their fractographic features are dimples for the bare specimen, and mixture of intergranular facets and dimples for the coated specimens.

TENSILE PROPERTIES

	UTS (ksi)	YS (ksi)	Elongation (%)
Bare	**298**	**247**	**13**
Coated with Cd and Ni Interlayer, Baked at 375ºF for 3 Days in Air	**299**	**246**	**13**

CONTROLLED UNCLASSIFIED INFORMATION

HYDROGEN EMBRITTLEMENT

Rising Step Load Test Result

The variation of threshold stress intensity for environmental hydrogen embrittlement (reference 7), $K_{th\text{-}EHE}$, and the net failure stress (reference 7), σ_{net}, with applied cathodic potential, V_{SCE}, is shown for the bare and coated M54 steel specimens in Figure A-4 and Table B-2. The $K_{th\text{-}EHE}$ is greatest for the bare specimen, and it is lost by coating. The loss is greater for the (Cd+Ni) coating than for the Cd coating. The $K_{th\text{-}EHE}$ of the coated specimen was found to increase with increasing baking period up to a certain one, but subsequently did not change with any further baking, as shown in Table B-3 and Figure A-5. In this case, the specimens were coated Cd with Ni interlayer, and they were baked in air for periods, ranging from 4 to 240 hours. The $K_{th\text{-}EHE}$ increased linearly* with the baking period to 150 ksi$\sqrt{n}$ after baking for 76 hours, and then did not change with any longer baking. (* The $K_{th\text{-}EHE}$ variation in the initial baking periods 4 to 76 hours can be expressed by an empirical linear equation, $K_{th\text{-}EHE} = 99.38 + 0.696t$, where t is the baking period.)

Slow Strain Rate Test Result

The result of the slow strain rate test for the M54 steel specimens, coated Zn-14% Ni with or without interlayer, is shown in Figure A-6. (In this case, no post-coating baking was done.) The plots indicate:

- In air, the fracture strength is reduced little with decreasing strain rate.
- In 3.5% NaCl solution, the decrease in fracture strength is more with decreasing strain rate, especially at strain rates below 10^{-6} s^{-1}.
- The fracture strength is less in 3.5% NaCl than in air for a given strain rate. [The difference is attributable to the hydrogen embrittlement in 3.5% NaCl solution.]
- The fracture strength in 3.5% NaCl solution is lower for the specimen coated (Zn-14%Ni) with Ni interlayer than for that without Ni interlayer. This result indicates that the Ni interlayer reduced the hydrogen embrittlement resistance more in 3.5% NaCl solution.

FATIGUE RESISTANCE

The results of the stress-life (S-N) fatigue tests for the M54 steels specimens, coated Cd with or without Ni interlayer, are shown in Figures A-7 and A-8. In air, the fatigue strength is reduced by coating with or without interlayer. Consequently, the fatigue resistance is greater for the bare specimen than for the coated one, Figure A-7(a). On the other hand, the reverse is true for the test in 3.5% NaCl solution, indicating the protective action of the coating against corrosion fatigue, Figure A-7(b). The fatigue resistances of the specimens coated Cd with or without Ni interlayer are similar in air and 3.5% NaCl solution, indicating a little or no effect of the Ni interlayer on the fatigue strength, Figures A-8(a) and (b).

Figures A-9, 10 and 11 show the typical SEM fractographs of the specimens, which were initially Cd with Ni interlayer coated, baked and then fatigue-tested. Cracks were initiated at four sites near the specimen surface and they grew inward. The largest one grew enough and formed both areas of slow crack growth and overload fracture, Figure A-9. Figure A-10 illustrates a

CONTROLLED UNCLASSIFIED INFORMATION

magnified fractograph with Cd coating, Ni interlayer and fracture surface morphology. From this figure, it is clear that the fatigue crack was initiated at a site on the interface between the Cd coating and Ni interlayer and grown inward through the Ni interlayer and substrate. Figure A-11 depicts striations in the slow crack growth area.

COATING THICKNESS

Coating Thickness (μm) was measured as follows.

Process	Cd	Ni Interlayer	Baking	Plating Procedure
1	**8**	**12**	**375ºF, 3 Hours, Air**	**Not Disclosed by Plater***
2	**6.5**	**9.6**	**375ºF, 3 Days, Air**	**Not Disclosed by Plater**

(* The coating work for this study was carried out by Programatic Platers, Inc. at Tenafly, NJ.)

CONTROLLED UNCLASSIFIED INFORMATION

DISCUSSION

Electrochemical Characteristics

The corrosion potential or open circuit potential -0.78v, determined for the Cd plus interlayer Ni coating, is less than that for the bare M54 steel -0.53v, as Figure A-2 shows. This confirms that the specimen coating is more active than the substrate M54 steel and it is sacrificial.

Fractographic Features for Bare & Coated Specimens

The fractographic feature for the bare specimen tested in air is dimples, as Figure A-3a shows. The dimple is typical of ductile fracture.

The fractographic feature, observed for the specimens coated Cd and Cd plus Ni interlayer and tested in air, is intergranular facets mixed with dimples, as Figures A-3b & 3c show. Since the intergranular facet and dimple are typical of hydrogen embrittlement and ductile fracture, respectively, the fracture of the coated specimens is partially attributed to the embrittlement by the hydrogen absorbed and trapped during the coating.

Loss of $K_{th\text{-}EHE}$ by Coating

Compared to the bare, both of the Cd coating and Cd plus Ni layer coating on M54 steel resulted in loss of $K_{th\text{-}EHE}$, as shown in Figure A-4 and Table B-1. The loss of $K_{th\text{-}EHS}$ is greater for the Cd plus Ni interlayer coating than for the Cd coating. Since $K_{th\text{-}EHS}$ is a measure of resistance to hydrogen embrittlement, the greater loss of $K_{th\text{-}EHS}$ indicates greater loss of resistance to hydrogen embrittlement for the Cd plus Ni interlayer coating. This is attributable to the blockage of egress and entrapment of more hydrogen by the Ni interlayer of low hydrogen diffusivity* in the specimen coated with Cd plus Ni interlayer than in the Cd coated one. [* The hydrogen diffusivity in Ni is reported to be $8x10^{-10}$ cm^2/s (reference 8).]

The lost $K_{th\text{-}EHE}$ at V_{SCE} = -0.6 volt for the Cd plus Ni interlayer coating was restored linearly with baking time to 150 ksi√in initially from 101 ksi√in for the bare but no more after 76 hours or longer baking, as Figure 5 and Table B-3 show. This is attributable to the residual or entrapped hydrogen, which was not releasable by the longer baking at 375°F in air. It has been reported that hydrogen can be trapped in various sites, such as carbide particles, dislocation cores, grain boundaries, and martensitic lathe boundaries (references 9-11). Scully (reference 11) reported that hydrogen trapped at higher trap binding energy sites was not removed by 374°F baking.

A number of researchers have studied the electroplating and baking. Some of their pertinent results are as follows. Cd electroplating produces a protective coating on steel surfaces that improves corrosion resistance, but atomic hydrogen (H) can be co-deposited during plating and may enter the steel substrate (references 12,13). A post-plating baking process is required to remove the residual H (references 12-17), however, the effectiveness has been questioned for ultra high strength steels, such as AISE 4340 (references 12,13,17). A coating can further complicate H egress/desorption during baking by acting as a diffusion barrier and H source. For electroplated Cd, H is co-deposited in both the Cd coating and steel substrate (reference 12,13,17). The H concentration in the steel increases during the early stage of baking with the

CONTROLLED UNCLASSIFIED INFORMATION

electroplated Cd layer serving as a H source, because the H solubility in Cd is higher than that in Fe (reference 12,13,17). The Cd layer also acts as a diffusion barrier during baking, due to the much slower H diffusion in Cd than in steel (reference 17). Hence, considerable diffusible H may remain in a baked steel, even after baking for 100 hours (reference 12). The 1-5 part-per-million by weight level of residual-dissolved H, typical of Cd plating and subsequent baking, embrittles AISE 4340 steel (reference 18). Similar problems were reported for Cd-plated steel fasteners (reference 19). There is limited information on which trap states govern hydrogen embrittlement compared to those that release H when baked at specified temperatures. Previous work demonstrated that weak trap sites provide a reservoir of mobile H that is capable of diffusing to the crack tip process zone and aggravate hydrogen embrittlement (references 20-22). There may be considerable residual H in higher energy trap sites after conventional baking treatment (reference 23). Whether such H repartitions to the hydrostatically stressed region ahead of a crack tip and facilitates embrittlement depends on the energetics of trapping at microstructural features. For a microstructure containing plentiful trap sites, it is necessary to consider the effectiveness of baking in removing hydrogen from various trap states (references 24,25). From these results, it is deducible that the Cd plus Ni interlayer coating provides greater blockage to H egress and more traps to hold H during post-coating baking than the Cd coating, resulting in greater loss of $K_{th\text{-}EHE}$.

SLOW STRAIN RATE TEST

Hydrogen Embrittlement Susceptibility Index

As Figures A-6(a) and (b) show, the fracture strength of a specimen becomes less in 3.5% NaCl solution than in air, noticeable more at a lower strain rate. The fracture strength reduction must be attributed to hydrogen embrittlement in 3.5% NaCl solution. The value normalized with the fracture strength in air can be a representative measure of susceptibility to hydrogen embrittlement. Therefore, a hydrogen embrittlement susceptibility index, I_{EHE}, is defined as

$$\mathbf{I_{EHE} = \Delta\sigma / \sigma_{air}} \quad \textbf{……(1)}$$

where

$\mathbf{\Delta\sigma = \sigma_{air} - \sigma_{NaCl}}$
$\mathbf{\sigma_{air}}$ **= fracture strength in air**
$\mathbf{\sigma_{NaCl}}$ **= fracture strength in NaCl solution**

The variation of the index with strain rate is shown in Figure A-12. This figure indicates that the hydrogen embrittlement susceptibility index, I_{EHE}, is greater for the coating of (Zn-14Ni) with Ni interlayer than for that of (Zn-14Ni), especially at lower strain rates.

From Figure A-6, it is clear that the Zn-14Ni and (Zn-14Ni) with Ni interlayer coated M54 steel specimens are not susceptible to hydrogen embrittlement in air under straining at rates, 10^{-7}–10^{-4} s^{-1}. This observation agrees with some other investigators'. Parkins (reference 26) reported no detectable SCC or hydrogen embrittlement of soft mild steel under straining at rates, 10^{-5} – 10^{-2}

CONTROLLED UNCLASSIFIED INFORMATION

s^{-1}, in air. Henry Holroyd and Scamans (reference 27) observed no SCC or hydrogen embrittlement occurring in 5083 H115 aluminum alloy at strain rates, 10^{-4} - 10^{-3} s^{-1}, in air. Yu et al (reference 28) found 70/30 brass unsusceptible to SCC or hydrogen embrittlement in air.

As shown in Figure A-12, in corrosive environments, the SCC or hydrogen embrittlement susceptibility index keeps increasing with decreasing strain rate from 10^{-4} to 10^{-7} s^{-1}. Similar observations were also made by some investigators (reference 26-28). Parkins (reference 26) found the SCC or hydrogen embrittlement susceptibility of mild steel in 1M NaH_2PO_4 at -1 V (SCE) increasing with decreasing strain rate from 10^{-2} to 10^{-6} s^{-1}. Yu et al (reference 28) found the susceptibility of 70/30 brass in 1M $NaNO_2$ increasing with decreasing strain rate from 10^{-3} to 10^{-7} s^{-1}. Holroyd (reference 27) noticed the susceptibility of 5050A wire in 3% NaCl + 0.3% H_2O_2 solution increasing with decreasing strain rate from 10^{-3} to 10^{-6} s^{-1}. However, the other investigators (reference 29-33) reported that the SCC or hydrogen embrittlement susceptibility, indicated by maximum load, area reduction, elongation or fracture energy, decreased after reaching the maximum at a strain rate, 10^{-5} s^{-1}, 10^{-6} s^{-1} or 10^{-7} s^{-1}.

CONTROLLED UNCLASSIFIED INFORMATION

CONCLUSIONS

- The corrosion potential or open circuit potential, -0.78v, determined for the Cd plus interlayer Ni coating, is less than that for the substrate M54 steel, -0.53V. This confirms that the coating is more active than the substrate M54 steel, and it is sacrificial.
- The fractographic features evidences that Cd and Cd plus Ni interlayer coatings induce partial embrittlement of the substrate M54 steel by hydrogen, absorbed and trapped during coating process.
- The coatings of Cd and Cd with Ni interlayer can protect the substrate M54 steel against corrosion fatigue in 3.5% NaCl solution.
- The susceptibility to hydrogen embrittlement is increased by Ni interlayer coating due to blockage of egress and entrapment of hydrogen by the Ni interlayer.
- Post-coating baking in air can prevent the hydrogen embrittlement of the coated M54 steel partially, but not completely.

CONTROLLED UNCLASSIFIED INFORMATION

REFERENCES

1. Elizabeth M. K. Hillier, "The Effect of Zinc-Cobalt Electroplating on the Hydrogen Embrittlement of High Strength Steel," PhD D Thesis, Cranfield University, U.K., July 2001.
2. Douglas J. Figueroa Gordon, "Hydrogen Re-Embrittlement Susceptibility of Ultra High Strength Steels," PhD D Thesis, Cranfield University, U. K., September 2005.
3. E. U. Lee, C. Lei, M. Stanley, B. Pregger, and C. Matzdorf, "Coated 4340," Report NAWCADPAX/TR-2013/252, Naval Air Warfare Center Aircraft Division, 2013.
4. E. U. Lee, M. Stanley, B. Pregger, C. Lei and E. Lipnickas, "Ferrium M54 Steel," Report NAWCADPAX/TIM-2014/292, Naval Air Warfare Center Aircraft Division, 2015.
5. Technical Bulletin, DIPSOL of America, Inc., Livonia, MI, June 1, 2013.
6. Rising Step-Load Test, ASM Handbook, Vol. 8, Mechanical Testing, ASM International, June 1995, pp. 539-40.
7. ASTM Standard F 1624-05, "Standard Test Method for Measurement of Hydrogen Embrittlement Threshold in Steel by the Incremental Step Loading Technique," ASTM International, 100 Barr Harbor Dr., West Conshohocken, PA 19428, Sept. 10, 2000.
8. T. M. Harris, "Hydrogen Diffusion and Trapping in Electrodeposited Nickel", PhD Thesis, MIT (1989).
9. J. P. Hirth, "Effects of Hydrogen on the Properties of Iron and Steel," *Metallurgical Transactions* A, Vol. 11A, June 1980, pp. 861-890.
10. S. Fernando, "Hydrogen Embrittlement & Stress Corrosion," Technical Note: AFI/02/006, AJAX Fasteners Innovations, Braeside VIC 3195, Australia, 03 July 2002, pp. 1-4.
11. J. R. Scully, H. Dogan, D. Li and R. Gangloff, "Controlling Hydrogen Embrittlement in Ultra-High Strength Steels," *Corrosion* 2004, Paper 04563.
12. J. B. Boody and V. S. Agawala, *Corrosion*/87, paper no. 224, NACE, Houston, TX, 1987.
13. D. A. Berman, *Materials Performance*, Vol. 24, pp. 36-41, 1985.
14. H. E. Townsend, *Corrosion*, Vol. 37, no. 2, pp. 115-20, 1981.
15. B950-98: Standard Guide for Post-Coating Treatment of Steel for Reducing Risk of Hydrogen Embrittlement, *Annual Book of ASTM Standards Vol. 02.05*, ASTM International, West Conshohocken, PA, pp. 613-5, 2001.
16. M. J. Robinson and R. M. Sharp, *Corrosion,* Vol. 41, no. 10, pp. 582-86, 1985.
17. T. Zhong-Zhuo, H. Chi-Mei, L. Rong-Bong, F. Yi-Feng, and C. Xiang-Rong, in *Current Solutions to Hydrogen Problems in Steels*, C. G. Interrante and G. M. Pressouyre, editors, ASM International, Materials Park, OH, pp. 98-103, 1982.
18. R. L. S. Thomas, "Internal Hydrogen Embrittlement of a Trap-Rich Ultra-High Strength Steel AerMet 100," MS Thesis, University of Virginia, Charlottesville, A, 2000.

CONTROLLED UNCLASSIFIED INFORMATION

19. E. L. Williams and D. M. Anderson, *Materials Performance*, Vol. 24, no. 12, pp.9-12, 1985.
20. R. P. Gangloff, in *Corrosion Prevention and Control*, M. Levy and S. Isserow, editors, U. S. Amy Materials Technology Laboratory, Watertown, MA, pp. 64-111, 1986.
21. M. Nagumo, M. Nakamura, and K, Takai, *Metallurgical and Materials Transactions A*, Vol. 32A, pp. 339-47, 2001.
22. G. M. Pressouyre and I. M. Bernstein, *Acta Metallurgica*, Vol. 27, pp. 89-100, 1979.
23. G. B. Olson, in *Innovation in Ultra-High Strength Steel Technology, 34th Sagamore Army Materials Conference*, US Army Laboratory Command, Watertown, MA, pp. 3-65, 1987.
24. G. M. Pressouyre, *Acta Metallurgica*, Vol. 28, pp. 895-911, 1980.
25. N. Suzuki, N. Ishii and T. Miyagawa, *Tetsu-to-Hagane (Journal of the Iron and Steel Institute of Japan)*, Vol. 82, no. 2, pp. 170-5, 1996.
26. R. N. Parkins: in *Environment-Sensitive Fracture: Evaluation and Comparison of Test Methods*, ASTM STP 821, S. W. Dean, E. N. Pugh, and G. M. Ugiansky, Eds., ASTM, Philadelphia, PA, 1984, pp. 5-31.
27. N. J. Henry Holroyd and G. M. Scamans: in *Environment-Sensitive Fracture: Evaluation and Comparison of Test Methods*, ASTM STP 821, S. W. Dean, E. N. Pugh, and G. M. Ugiansky, Eds., ASTM, Philadelphia, PA, 1984, pp. 202-241.
28. J. Yu, N. J. Henry Holroyd, and R. N. Parkins: in *Environment-Sensitive Fracture: Evaluation and Comparison of Test Methods*, ASTM STP 821, S. W. Dean, E. N. Pugh, and G. M. Ugiansky, Eds., ASTM, Philadelphia, PA, 1984, pp. 288-309.
29. C. D. Kim and R. F. Wilde: in *The Slow Strain Rate Technique*, G. M. Ugiansky and J. H. Payer, eds., ASTM STP 665, ASTM, Philadelphia, PA, 1979, pp. 97-112
30. Buhl: in *Stress Corrosion Cracking – The Slow Strain Rate Technique*, G. M/ Ugiansky and J. H. Payer, eds., ASTM STP 665, ASTM, Philadelphia, PA, 1979, pp. 333-46.
31. G. M. Ugiansky, C. E. Johnson, D. S. Thompson and E. H. Gillespie: in *Stress Corrosion Cracking – The Slow Strain-Rate Technique*, ASTM STP 665, G. M. Ugiansky and J. H. Payer, eds., ASTM, Philadelphia, PA, 1979, pp. 254-65.
32. R. N. Parkins: in *The Slow Strain Rate Technique*, M. Ugiansky and J. H. Payer, eds., ASTM, STP 665, ASTM Philadelphia, PA, 1979, pp. 5-25.
33. M. Khobaib and C. T. Lynch: in *Environment-Sensitive Fracture: Evaluation and Comparison of Test Methods*, ASTM STP 821, S. W. Dean, E. N. Pugh, and G. M. Ugiansky, Eds., ASTM, Philadelphia, PA, 1984, pp. 242-255.

APPENDIX A
FIGURES

CONTROLLED UNCLASSIFIED INFORMATION

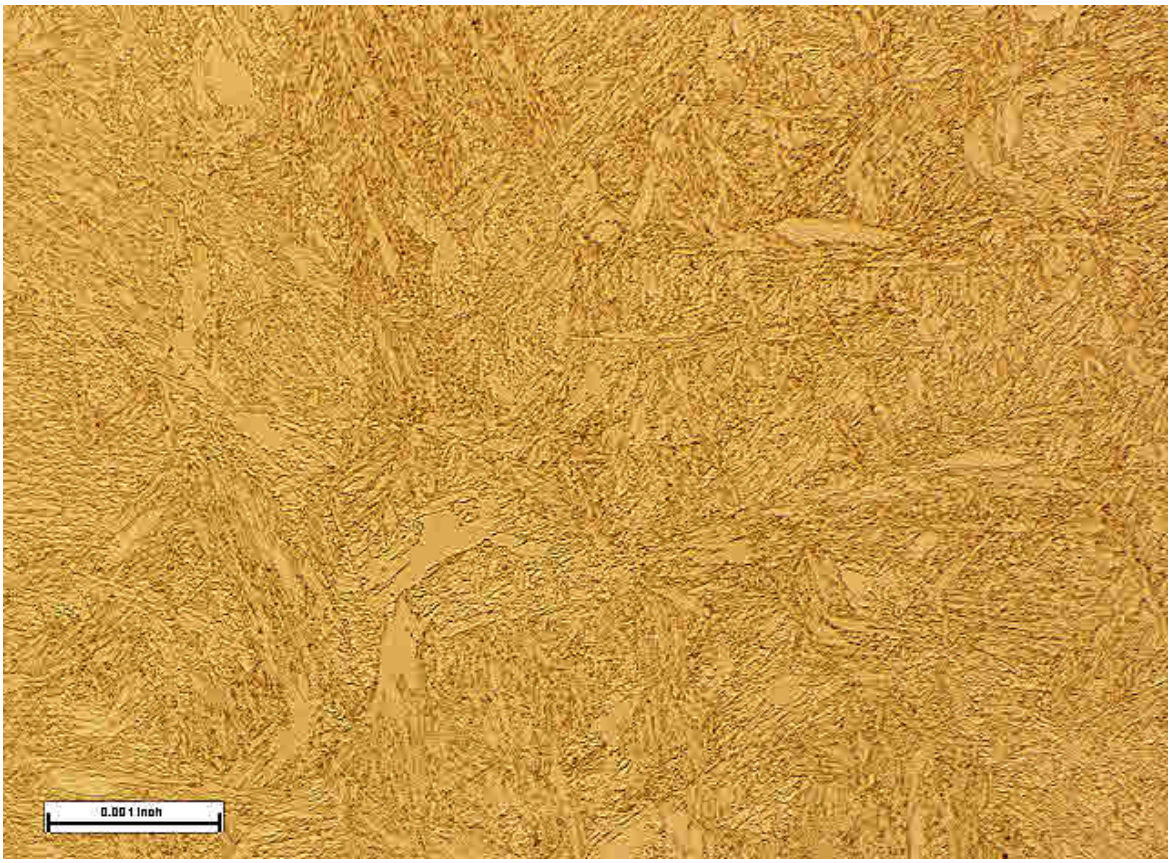

Figure A-1: Microstructure of Ferrium M54 Steel

CONTROLLED UNCLASSIFIED INFORMATION

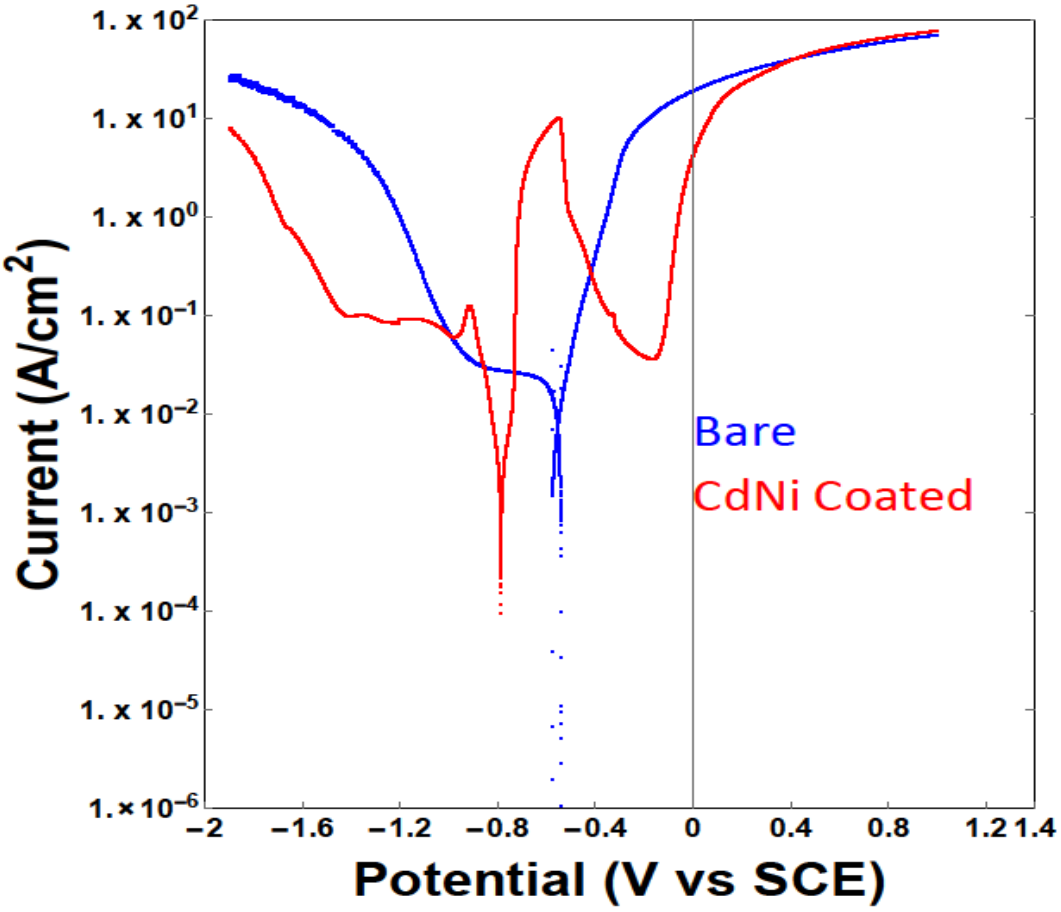

Figure A-2 : Polarization Plots of Bare & Cd with Ni Interlayer Coated M54 Steel [Corrosion Potential: Bare -0.53v, Cd with Ni Interlayer Coated -0.78v]

CONTROLLED UNCLASSIFIED INFORMATION

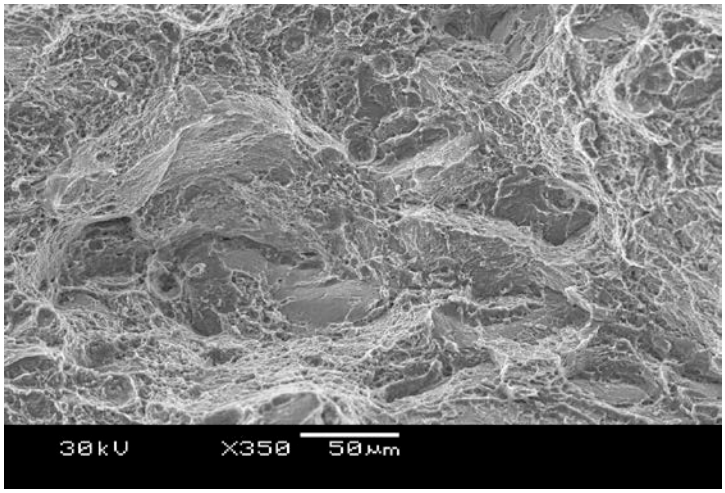

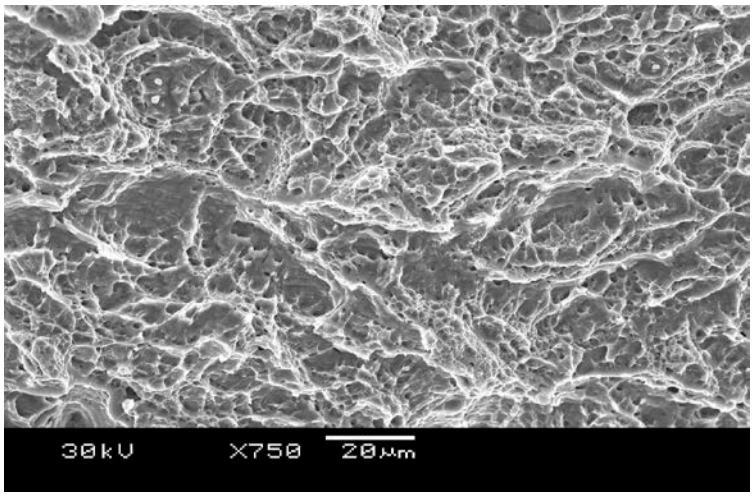

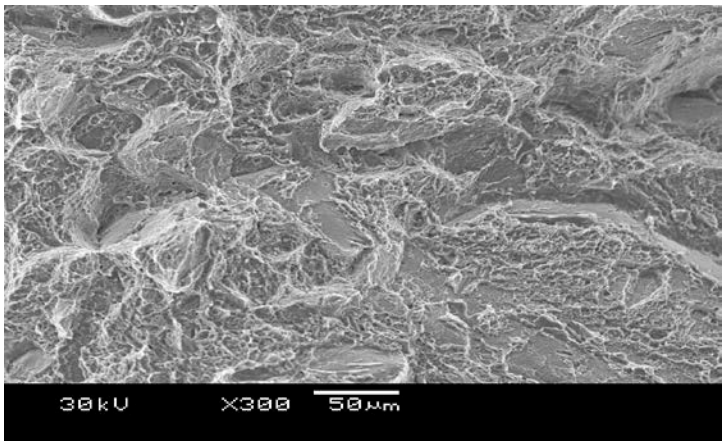

Cd & Ni Interlaver Coated

Figure A-3: SEM Fractographs of Bending Fracture of Coated M54 Steel Specimen

CONTROLLED UNCLASSIFIED INFORMATION

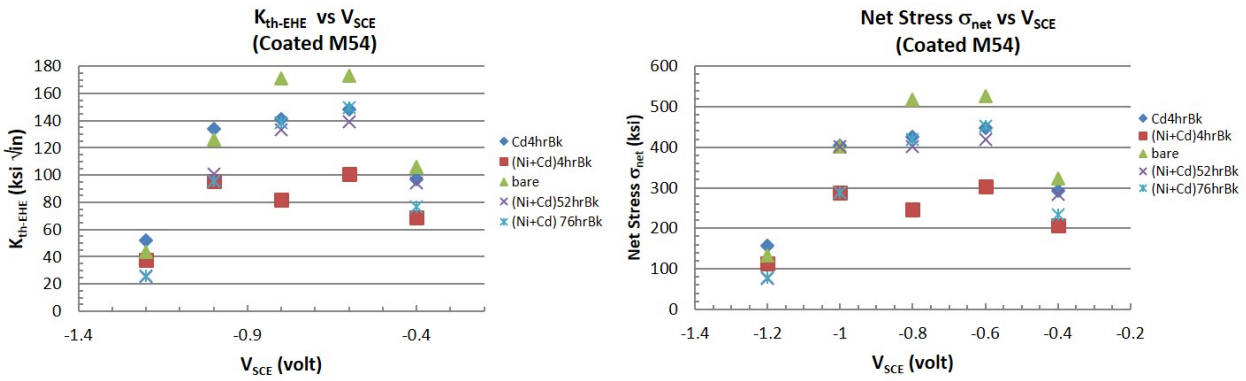

Figure A-4: Variation of $K_{th\text{-}EHE}$ & σ_{net} with V_{SCE} for Bare & Coated M54 Steel

CONTROLLED UNCLASSIFIED INFORMATION

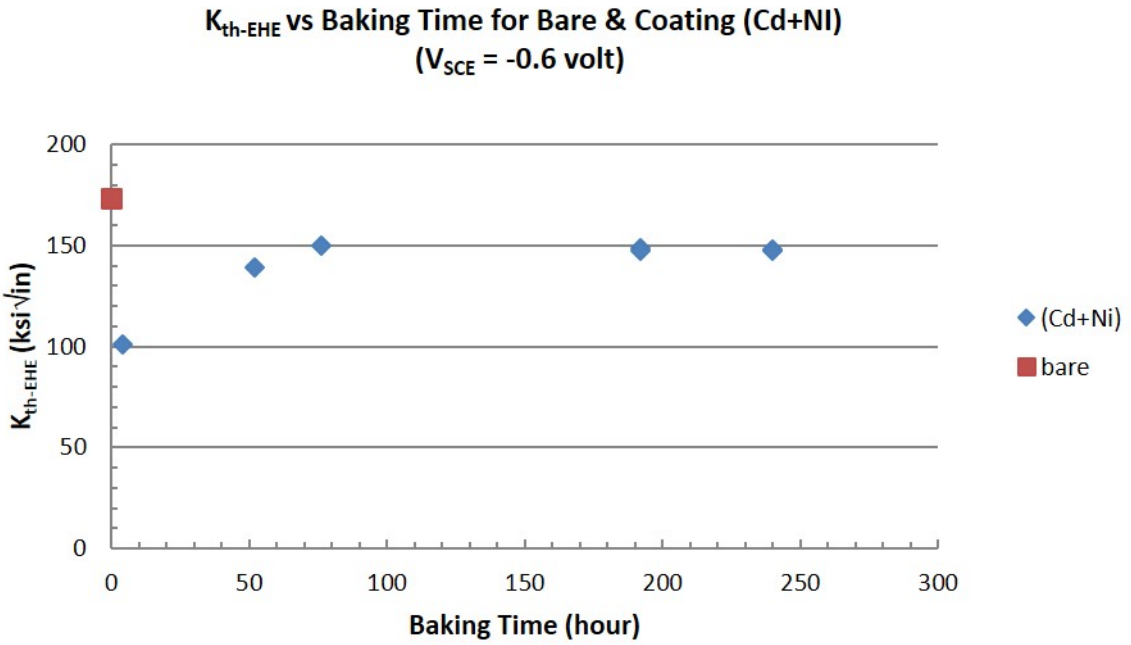

Figure A-5: Variation of $K_{th\text{-}EHE}$ with Baking Time for Bare & Cd with Ni Interlayer Coated M54 Steel

CONTROLLED UNCLASSIFIED INFORMATION

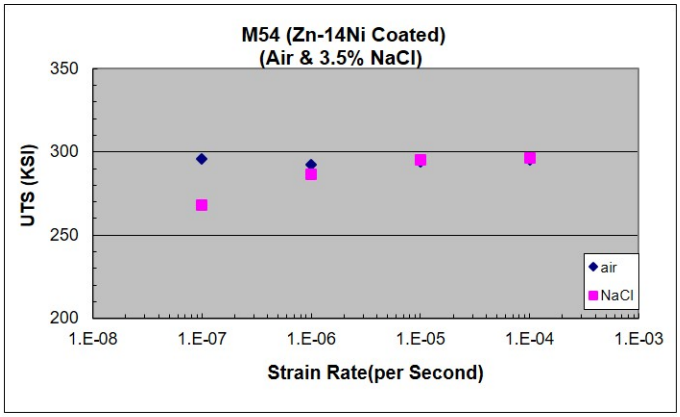

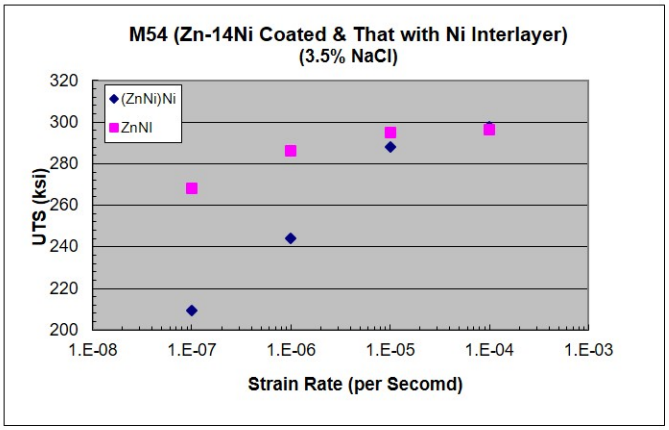

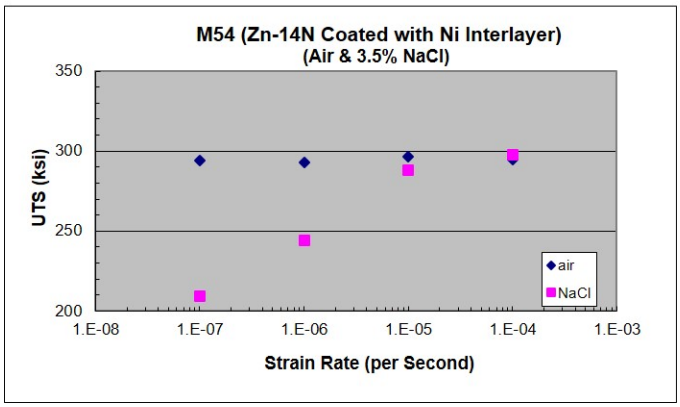

(ZnNi)Ni: Coated (Zn-14Ni) with Ni Interlayer
ZnNi: Coated (Zn-14Ni)

Figure A-6: Variation of UTS with Strain Rate in Air & 3.5% NaCl Solution for (Zn-14% Ni) with or without Ni Interlayer Coated M54 Steel

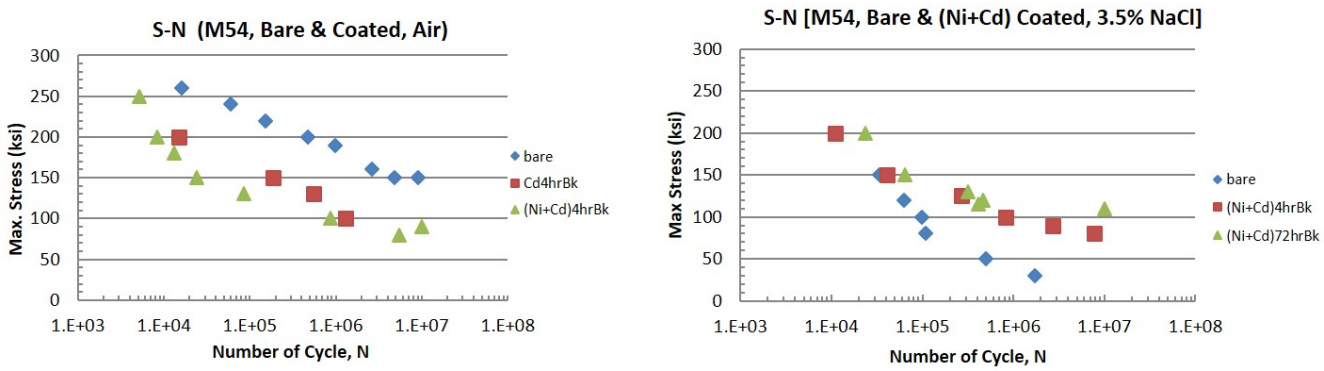

Figure A-7: Stress-Life Fatigue Curve of M54 Steel, Bare & Cd Coated with or without Ni Interlayer

CONTROLLED UNCLASSIFIED INFORMATION

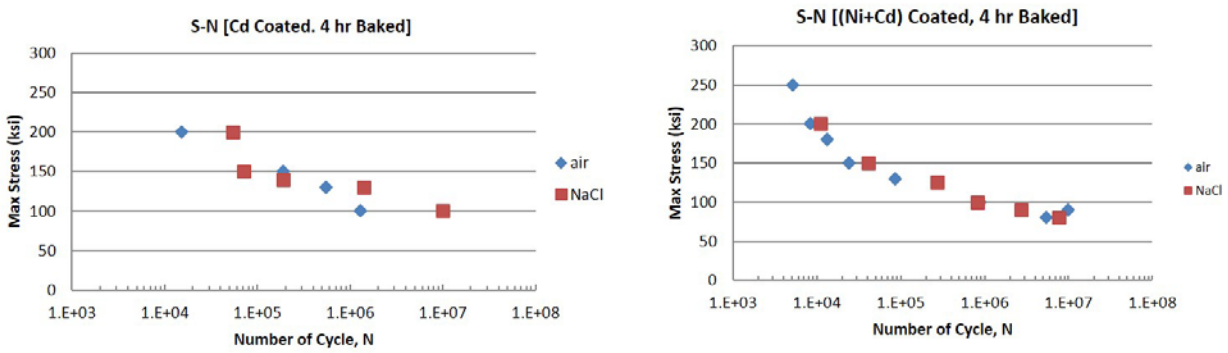

Figure A-8: Stress-Life Fatigue Curve of M54 Steel, Cd Coated with or without Ni Interlayer

CONTROLLED UNCLASSIFIED INFORMATION

Figure A-9: SEM Fractograph of M54 Steel, Cd Coated with Ni Interlayer and Stress-Life Fatigue-Tested in Air

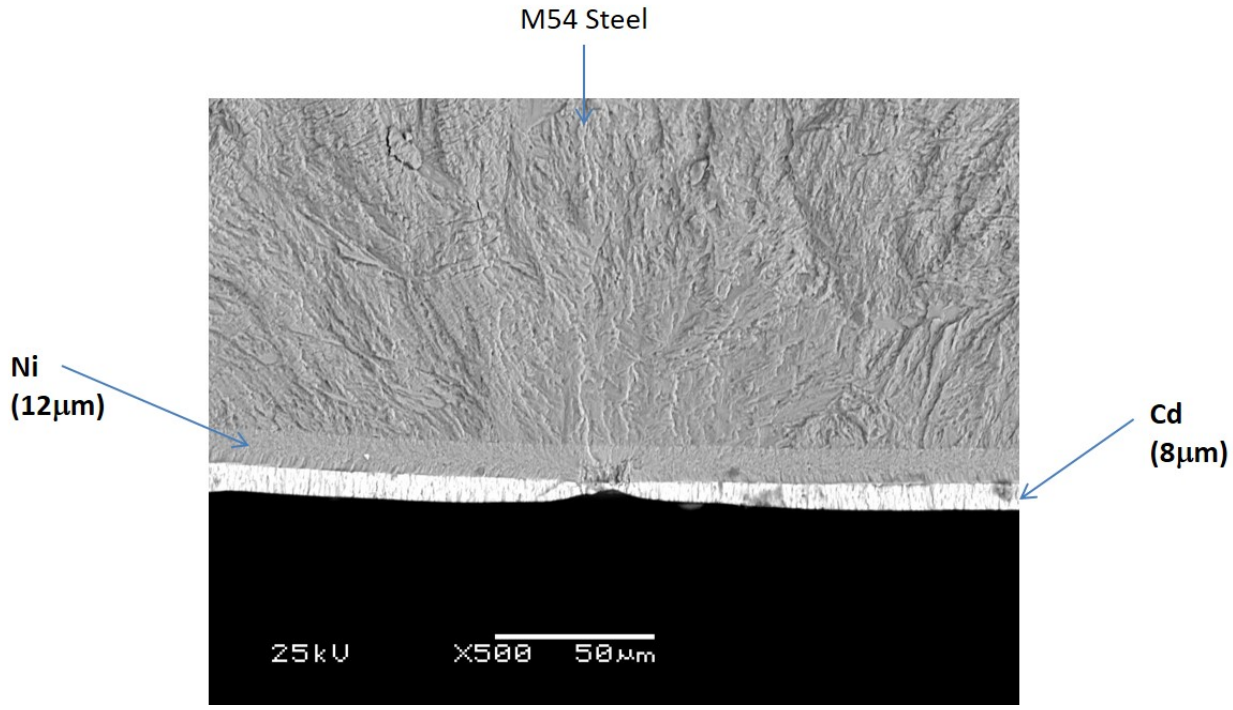

Figure A-10: SEM Fractograph of M54 Steel, Cd Coated with Ni Interlayer and Stress-Life Fatigue-Tested in Air, showing Cross-Sections of Coating Layers

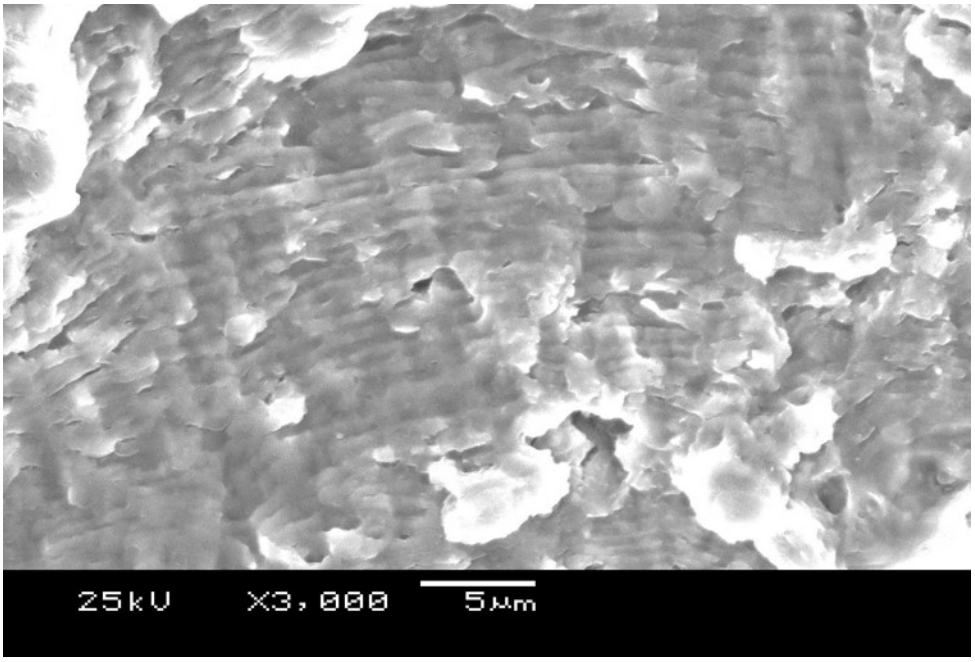

Figure A-11: SEM Fractograph of M54 Steel, Cd Coated with Ni Interlayer and Stress-Life Fatigue-Tested in Air, showing Striations

CONTROLLED UNCLASSIFIED INFORMATION

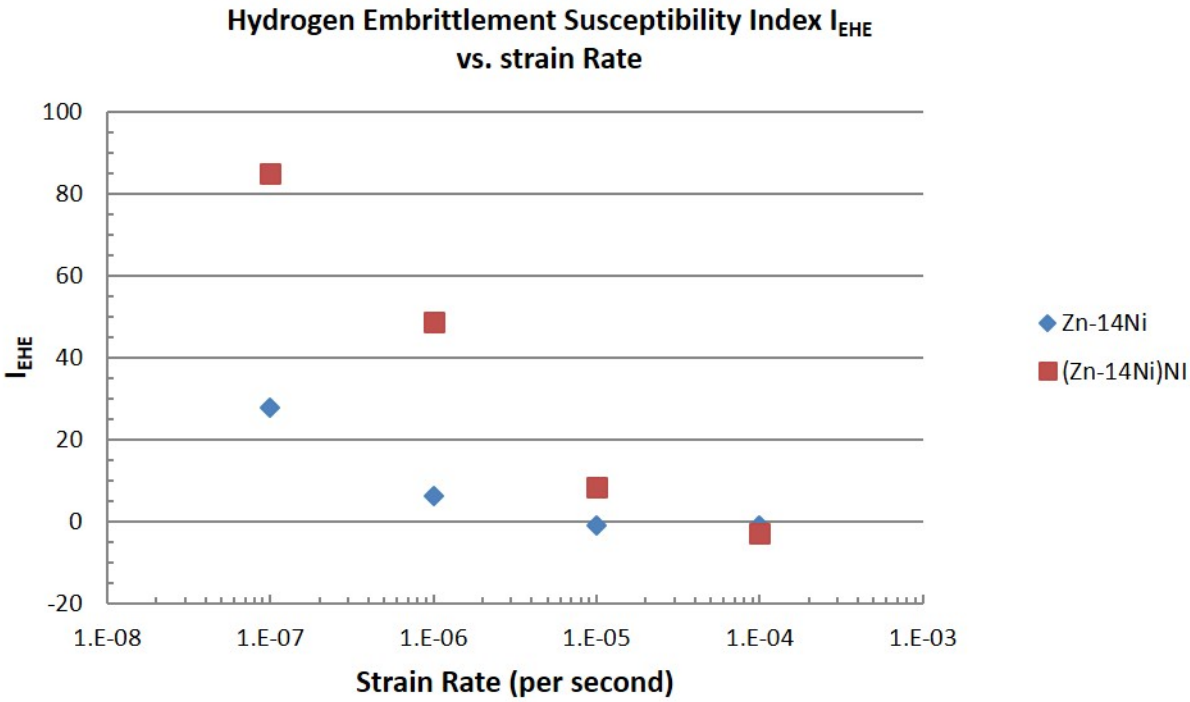

Figure A-12: Variation of Hydrogen Embrittlement Susceptibility Index with Strain Rate for M54 Steel, (Zn-14% Ni) Coated with or without Ni Interlayer

THIS PAGE INTENTIONALLY LEFT BLANK

APPENDIX B
TABLES

Table B-1: Chemical Composition (wt%) of M54 Steel

C	Cr	Ni	Mo	Co	V	W	Fe
0.30	**1.00**	**10.00**	**2.00**	**7.00**	**0.10**	**1.30**	**balance**

Table B-2: $K_{th\text{-}EHE}$ & Net Bending Stress Values at V_{SCE} = -0.6 volt in 3.5% NaCl Solution for M54 Steels, Bare, and Coated with Cd and (Cd+Ni)

Specimen	$K_{th\text{-}EHE}$ (ksi√in)	$\Delta K_{th\text{-}EHE}$ (ksi√in)	σ_{net} (ksi)	$\Delta\sigma_{net}$ (ksi)
Bare	**173**	**0**	**526**	**0**
(Cd+Ni), 76 Hr Bk	**150**	**-24**	**453**	**-73**
Cd, 4 Hr Bk	**148**	**-25**	**447**	**-78**
(Cd+Ni), 52 Hr Bk	**139**	**-34**	**420**	**-106**
(Cd+Ni), 4 Hr Bk	**101**	**-72**	**304**	**-222**

Table B-3: Variation of $K_{th\text{-}EHE}$ with Baking Time at V_{SCE} = -0.6 volt

Baking Time (hr)	$K_{th\text{-}EHE}$ (ksi√in)
4	**101**
52	**139**
76	**150**
192	**148**
192	**148**
240	**148**

CONTROLLED UNCLASSIFIED INFORMATION

DISTRIBUTION:

NAVAIRSYSCOM (Dr. James Sheehy), Bldg. 2109, Room N122 (1)
48150 Shaw Road, Patuxent River, MD 20670

NAVAIRSYSCOM (Ms. Kristi Wiegman), Bldg. 2109 (1)
48150 Shaw Road, Patuxent River, MD 20670

NAVAIRSYSCOM (Colin Wilkenson), Bldg. 2187, Suite 3322 (1)
48110 Shaw Road, Patuxent River, MD 20670-1906

NAVAIRSYSCOM (John Brennan), Bldg. 2188 (1)
48066 Shaw Road, Patuxent River, MD 20670-1908

NAVAIRSYSCOM (Robert Kowalik), Bldg. 2188 (25)
48066 Shaw Road, Patuxent River, MD 20670-1908

FRC/ISSC Jacksonville (John Benfer) (1)
Naval Air Station, Jacksonville, FL 32212

NAVAIRWARCENACDIV (4.12.6.2), Bldg. 407, Room 116 (1)
22269 Cedar Point Road, Patuxent River, MD 20670-1120

NAVAIR (AIR-4.0T – Tech. Library), Bldg. 407, Room 116, Patuxent River, MD

DTIC, 8725 John J. Kingman Road, Suite 0944, Ft. Belvoir